Journal of Solid State Chemistry 215 (2014) 171–175

Contents lists available at ScienceDirect

Journal of Solid State Chemistry

journal homepage: www.elsevier.com/locate/jssc

Magnetic ordering in the pyrochlore Ho_2CrSbO_7 determined from neutron diffraction, and the magnetic properties of other RE_2CrSbO_7 phases (RE=Y, Tb, Dy, Er)

Mariana J. Whitaker [1], Colin Greaves *

School of Chemistry, University of Birmingham, Birmingham B15 2 TT, UK

ARTICLE INFO

Article history:
Received 31 January 2014
Received in revised form
26 March 2014
Accepted 30 March 2014
Available online 8 April 2014

Keywords:
Pyrochlore
Neutron diffraction
Magnetic structure
Spin-ice
Holmium

ABSTRACT

The magnetic structure of the pyrochlore Ho_2CrSbO_7, which orders magnetically below 13 K, has been studied using neutron powder diffraction. Ho_2CrSbO_7 is found to form an "ordered spin-ice structure" where the magnetic moments are constrained along the 111 axes, but with a ferromagnetic moment in one direction. The Cr^{3+} ions order ferromagnetically and this is thought to lift the degeneracy of the x, y and z directions in the cubic structure causing the ferromagnetic component from the Ho^{3+} ions to align. The pyrochlores RE_2CrSbO_7 where RE=Y, Tb, Dy and Er have also been prepared and studied using SQUID magnetometry.

1. Introduction

Mixed metal oxides with the pyrochlore structure are of considerable interest because of their susceptibility to chemical modifications which gives rise to a wide range of possible compositions and useful properties [1,2]. Their structure is based on the mineral pyrochlore, $NaCaNb_2O_6F$, and has cubic symmetry (space group $Fd\bar{3}m$) with a lattice parameter, a, of around 10 Å. The structure can be represented using the general formula $A_2B_2O_7$ (or $A_2B_2O_6O'$ to distinguish the presence of two different oxygen anions) where the A-cation is larger and 8-coordinate, typically a rare earth or large lone pair cation, and the B-cation is smaller and 6-coordinate, usually a transition metal or metallic p-block element. There are two principal ways of describing the pyrochlore structure: it can be viewed as two networks of BO_6 octahedra and A_2O' chains and also as an oxygen deficient fluorite superstructure. Substitutions can be made at the *A*-, *B*- and *O*-sites and ions of the same element can also be distributed over both the *A*- and *B*-sites giving a variety of different pyrochlores with many diverse properties. This includes insulators, semiconductors and metals, and superconductivity has been observed in some compounds [3,4]; piezoelectrics, dielectrics and ferroelectrics are also found [1].

The pyrochlore structure is interesting magnetically because it contains two interlinked sublattices of A and B corner-sharing tetrahedra (Fig. 1) and if one or both of the cations are magnetic this leads to highly frustrated systems with interesting and unusual magnetic properties [5]. Often this frustration prevents long-range ordering of the magnetic moments and spin-glass behaviour is seen, where the random arrangement of the moments is frozen in at low temperatures, but there are also pyrochlores which show transitions to long-range ordered, antiferromagnetic and ferromagnetic, states and pyrochlores with more exotic types of magnetic behaviour such as spin-liquids and spin-ices [5,6].

The spin-ice magnetic state was first observed for the pyrochlore oxide $Ho_2Ti_2O_7$ [7]. The magnetic moments are constrained along the crystallographic directions and order only at very low temperatures so that in any given tetrahedron two of the spins are pointing in to, and two are pointing out from, the centre of the tetrahedron (Fig. 2). As the x, y and z directions in a cubic structure are equivalent there is no preferred direction for the spins to align along, unless a field is applied, giving a macroscopically degenerate ground state [6]. This is closely related to the residual entropy arising from the arrangement of protons in hexagonal water ice [8]: each oxygen atom is tetrahedrally surrounded by four hydrogen atoms and forms two short and two long O–H bonds (Fig. 2). The spin-ice pyrochlores are of interest because their structure has been suggested as a host for magnetic monopoles [9].

* Corresponding author.
E-mail address: c.greaves@bham.ac.uk (C. Greaves).
[1] Current address: Department of Chemistry and Chemical Biology, Rutgers University, Piscataway, NJ 08854, USA

http://dx.doi.org/10.1016/j.jssc.2014.03.039

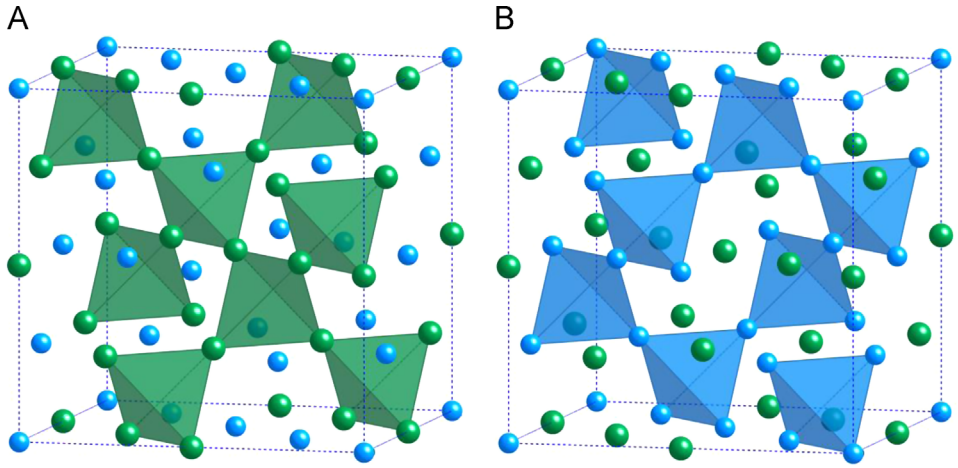

Fig. 1. Pyrochlore structure showing the tetrahedral arrangement of A-cations (green) and B-cations (blue). Oxygen anions are not shown. (For interpretation of the references to colour in this figure legend, the reader is referred to the web version of this article.)

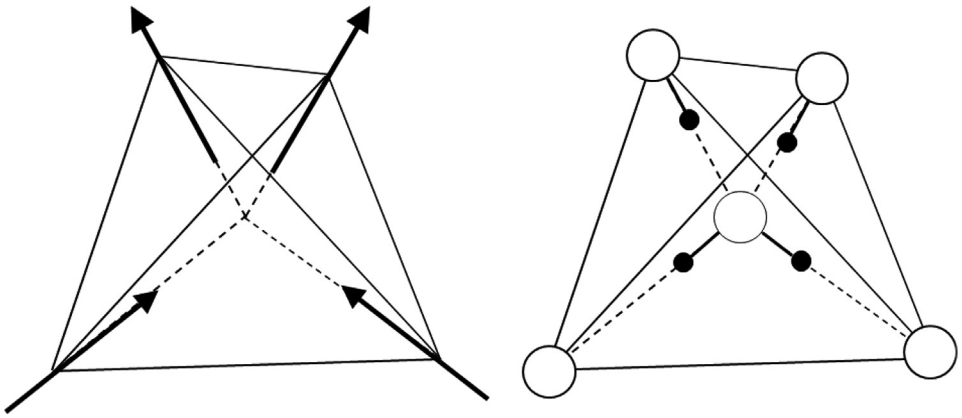

Fig. 2. Arrangement of magnetic spins for a given tetrahedron in a spin ice structure (left) and the arrangement of hydrogen ions in water ice (right): oxygen ions are shown as large white spheres and hydrogen ions are shown as small black spheres.

Despite the magnetic frustration inherent within the cation sublattices of the pyrochlore structure, a previous study of the magnetic susceptibility and magnetisation of RE_2CrSbO_7 found the compounds Ho_2CrSbO_7 and Dy_2CrSbO_7 to be ferromagnetic below $T_c = 10$ K and 16 K respectively [10]. Given the spin-ice magnetic behaviour of, for example, $Ho_2Ti_2O_7$, the reason for a ferromagnetic ground state in these phases with mixed Cr^{3+} and Sb^{5+} on the B-sites has not been established and prompted the current investigation. Here we report magnetic data for the pyrochlores RE_2CrSbO_7 (RE=Y, Tb, Dy, Ho, Er) and the magnetic structure of Ho_2CrSbO_7 as determined from neutron powder diffraction data. The magnetic structures of the compounds have not previously been reported.

2. Experimental

Ho_2CrSbO_7 was prepared by heating stoichiometric amounts of Ho_2O_3 ($\geq$ 99.9%), Cr_2O_3 (99%) and Sb_2O_4 powders in air for 3 days at 950 °C and then regrinding and reheating at 1200 °C for 4.5 days with several intermediate regrindings. Sb_2O_4 was prepared by heating Sb_2O_3 (99%) in air at 640 °C.

Y_2CrSbO_7, Tb_2CrSbO_7, Dy_2CrSbO_7 and Er_2CrSbO_7 were prepared by heating stoichiometric amounts of $CrSbO_4$ and RE_2O_3 (99.9%–99.99+%) powders in air for 5.5 days at 1200 °C with one intermediate regrind. $CrSbO_4$ was prepared by heating Cr_2O_3 (99%) and Sb_2O_3 (99%) in air for 7 days at 1200 °C; several intermediate regrindings with addition of excess Sb_2O_3 were necessary to compensate for a loss of Sb_2O_3 due to volatilisation.

X-ray powder diffraction data were collected at room temperature using a Bruker D8 diffractometer (Cu $K\alpha_1$ radiation, wavelength 1.5406 Å; Ge crystal monochromator) operating in transmission mode, using a moveable 3° 2θ position sensitive detector and a step size of approximately 0.02°.

Constant wavelength neutron powder diffraction (NPD) data were collected using the high-resolution powder diffractometer for thermal neutrons (HRPT) at the neutron source SINQ at the Paul Scherrer Institute in Switzerland. Diffraction patterns were recorded at 300 and 1.5 K at a wavelength of 1.8857 Å.

Rietveld refinements were performed on both the X-ray and neutron diffraction data using the General Structure Analysis System (GSAS) [11] and the graphical user interface EXPGUI [12].

Magnetisation measurements were performed using a Quantum Design MPMS SQUID magnetometer. Zero-field cooled (ZFC) and field cooled (FC) data were collected between 5 and 300 K using an applied fields between 100 and 5000 Oe. Hysteresis measurements for Ho_2CrSbO_7 and Dy_2CrSbO_7 were taken between −500 and 500 Oe at 5 K. A small sample size (approximately 6 mg) had to be used as the lanthanide and moments were too large to give good quality hysteresis data when using a sample size of around 60–80 mg. Hysteresis measurements for Y_2CrSbO_7 were taken between −48,000 Oe and 48,000 Oe at 5 K.

3. Results and discussion

3.1. Structural characterisation

All the compounds were confirmed to be single phase using X-ray powder diffraction. Rietveld refinements were performed on the X-ray diffraction data using the general structure for a pyrochlore which has cubic space group $Fd\bar{3}m$, the $O1$ x value being the only variable in the atomic positions. The unit cell sizes, $O1$ x values and thermal parameters are shown in Table 1. A Rietveld refinement performed on room temperature neutron diffraction data for the compound Ho_2CrSbO_7 (Fig. 3) gave values of $a=10.1739(3)$ Å and $O1$ $x=0.3318$ ($\chi^2=1.924$; $R_{wp}=0.040$; $R_{F^2}=0.039$). The data fit to the model very well and the Cr/Sb ratio was found to be approximately 1:1 as expected.

3.2. Magnetic properties of Ho_2CrSbO_7.

3.2.1. Fully ordered region (below 13 K).

The presence of a magnetically ordered state was evidenced by a transition in the magnetic susceptibility data at ca. 13 K (Fig. 4)

Table 1
Structural parameters refined from powder X-ray diffraction data from RE_2CrSbO_7.

Compound	a (Å)	$O1$ x	U_{iso} (Å^2)	χ^2
Y_2CrSbO_7	10.1621(1)	0.3466(6)	0.0057(3)	1.921
Tb_2CrSbO_7	10.2199(1)	0.3315(6)	0.0114(4)	1.847
Dy_2CrSbO_7	10.1954(1)	0.3319(6)	0.0104(3)	1.364
Ho_2CrSbO_7	10.17503(9)	0.3365(5)	0.0070(3)	1.800
Er_2CrSbO_7	10.1464(1)	0.3329(6)	0.0112(3)	2.838

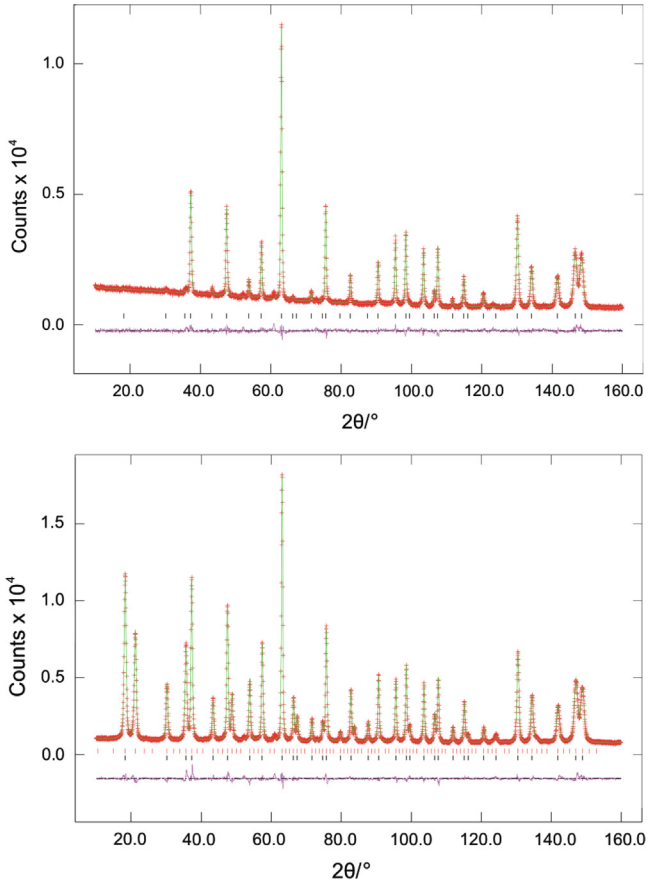

Fig. 3. Observed, calculated and difference plots for NPD data from Ho_2CrSbO_7 recorded at 298 K (above) and 1.5 K (below).

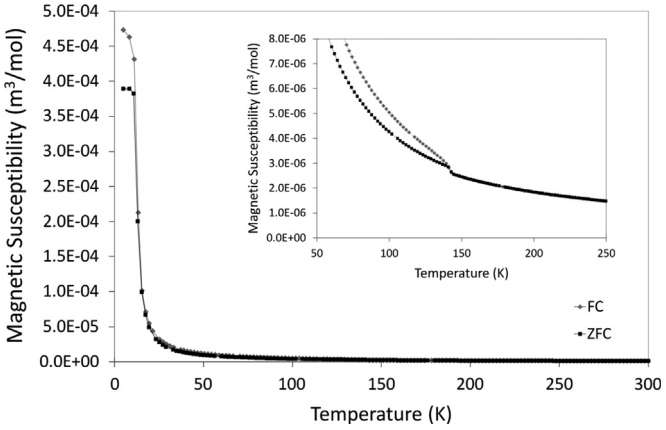

Fig. 4. Variation of magnetic susceptibility with temperature for Ho_2CrSbO_7 at an applied field of 500 Oe. Inset: magnetic susceptibility of Ho_2CrSbO_7 between 50 and 250 K.

and by the appearance of additional magnetic Bragg peaks in NPD data at low temperatures (Fig. 3).

In the magnetic susceptibility data (see Fig. 4), an increase in the susceptibility is seen at low temperatures with divergence of the FC and ZFC data indicative of a ferromagnetic component. The inset of Fig. 4 reveals a weak magnetic transition at 146 K. This was shown to be caused by a very small impurity of $HoCrO_3$, which orders to give a canted antiferromagnetic structure below this temperature [13]. Some very small $HoCrO_3$ impurity peaks were also seen in the NPD data (Fig. 3). Ho_2CrSbO_7 contains two different magnetic ions: Ho^{3+} on the A-sites and Cr^{3+} occupying half the B-sites.

The neutron diffraction pattern taken at 1.5 K (Fig. 3) revealed that Ho_2CrSbO_7 is not a simple ferromagnet. The nuclear structure was refined with space group $Fd\bar{3}m$ and the magnetic structure was refined as a separate phase with P1 symmetry such that the directions of the moments were unrestricted. Moments were initially input for the Ho^{3+} ions on the A-sites with a component aligned along one axis only, similar to the magnetic model for the antiferromagnetic pyrochlore $Er_2Ru_2O_7$ [14] which also has magnetic A- and B-sites. Neither a simple ferromagnetic nor an antiferromagnetic structure would allow all the magnetic peaks to be modelled. Looking at the low temperature neutron diffraction pattern of Ho_2CrSbO_7, it appeared similar to that of the pyrochlore $Tb_2Sn_2O_7$ taken at 0.1 K [15]. $Tb_2Sn_2O_7$ is a spin-liquid which undergoes a transition at 0.87 K to an ordered spin-ice state with both ferromagnetic and antiferromagnetic orders [15]. Therefore a model with antiferromagnetic ordering along two axes, x and y, and a ferromagnetic component along the third axis, z, was tested which modelled all the peaks. The moments were constrained to be along the $\langle 111 \rangle$ axes to give an ordered spin ice model.

The contribution from Cr^{3+} ions to the magnetic reflections was expected to be small due to the much larger Ho^{3+} moment and the Ho:Cr ratio of 2:1. The Cr^{3+} ions occupy half the B-sites and the magnetic interactions between them are diluted by non-magnetic Sb^{5+} ions. Various Cr ordering models were tested and a model with ferromagnetic ordering of the Cr^{3+} ions was seen to give a significantly better fit. The arrangement of magnetic moments on the Ho and Cr tetrahedra is shown in Fig. 5. The final magnetic model gave Ho^{3+} moments along the x, y and z axes of 5.78(3) μ_B, resulting in a total Ho^{3+} moment of 10.02(5) μ_B, and a Cr^{3+} moment of 2.72(5) μ_B ($\chi^2=2.978$; $R_{wp}=0.042$; $R_{F^2}=0.020$). The Ho^{3+} moment is in excellent agreement with the expected moment of 10.0 μ_B; the reduction in the Cr^{3+} moment the ideal value of 3.0 μ_B primarily relates to covalence effects. The unit cell contracts at low temperature as expected giving an a-parameter at 1.5 K of 10.1648(1) Å.

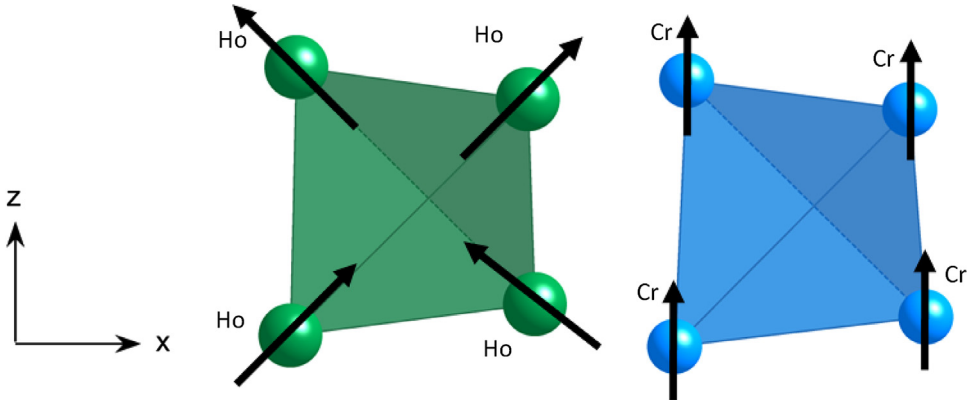

Fig. 5. Representations of the magnetic structure of Ho_2CrSbO_7 showing the arrangement of magnetic moments on single Ho and Cr tetrahedra. The Ho^{3+} moments are pointing in and out from the centre of the tetrahedron along ⟨111⟩ directions and the Cr^{3+} ions only occupy half of the *B*-sites.

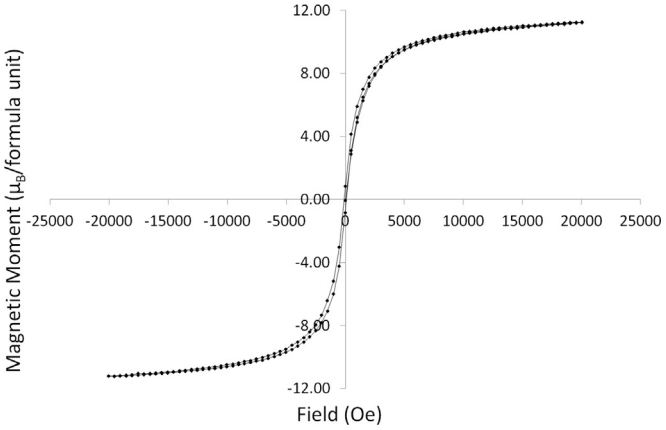

Fig. 6. Isothermal (5 K) field sweep magnetisation data for Ho_2CrSbO_7.

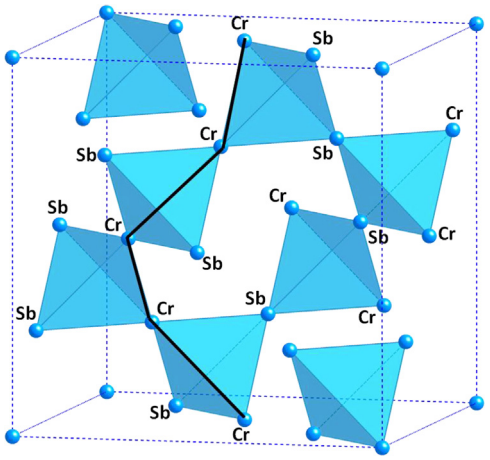

Fig. 7. Diagram showing the way in which Cr^{3+} ions could form magnetically linked chains throughout the pyrochlore structure.

Hysteresis data were collected below the magnetic ordering transition, at 5 K (Fig. 6). The saturated moment obtained from the plot was 11.2 μ_B per formula unit, much lower than the value of 23 μ_B expected for complete alignment of the moments on all the magnetic ions. However, reduced moments for the lanthanide ions in these types of pyrochlore have been seen previously due to a local ⟨111⟩ Ising anisotropy [7,15–17]. The full moment cannot be seen because the magnetic moments are constrained along the ⟨111⟩ axes and the field applied is too weak to turn them away from this direction. Assuming the moments lie along the ⟨111⟩ axes with the ferromagnetic component in the *z*-direction, the reduced moment observed in the *z*-direction is calculated to be 5.8 μ_B. This gives a total calculated saturated moment of 14.6 μ_B which is much closer to the observed value of 11.2 μ_B. The calculated value is still too high but would be expected to be reduced further due to the average arrangement of the crystallites in a powder sample.

The presence of magnetic Ho^{3+} ordering in this highly frustrated magnetic system and the breaking of cubic magnetic symmetry is interesting and suggests that there must be an influence from the magnetic *B*-site ions. The related compound Ho_2FeSbO_7 was also prepared and shown to be paramagnetic at all temperatures. This suggests that the Cr^{3+} ions are crucial in inducing magnetic order in the systems. Mixed compounds $Ho_2Cr_{1-x}Fe_xSbO_7$ ($x=0.25$, 0.5, and 0.75) were also prepared and magnetic ordering at low temperatures was indicated from preliminary SQUID magnetometry data showing that even small amounts of Cr ($x=0.25$) can induce a ferromagnetic transition. The *B*-sites are 50% occupied by Cr^{3+} ions and 50% occupied by Sb^{5+} ions; therefore a given B_4 tetrahedron is likely to contain two Cr^{3+} ions and two Sb^{5+} ions. The B_4 tetrahedra are corner linked and the Cr^{3+} ions can interact magnetically through 130° Cr–O–Cr links. Each Cr^{3+} would therefore have two Cr^{3+} neighbours it could interact with forming magnetically linked Cr^{3+} chains throughout the structure (Fig. 7). It is likely that such chains are responsible for the ferromagnetic ordering of the Cr^{3+} ions, which induces the ferromagnetic moments on the Ho^{3+} ions to be along a single axis, here assumed to be *z* (Fig. 5).

3.2.2. *Paramagnetic region.*

The inverse susceptibility data above $T=150$ K can be fitted to the Curie–Weiss law giving a total moment, $\mu_{total}=15.4$ μ_B and a Weiss constant, $\theta=-3.4$ K. The moment is almost exactly as expected for two Ho^{3+} ions ($\mu_{exp}=10.60$ μ_B) and one Cr^{3+} ion ($\mu_{spin\ only}=3.87$ μ_B). The negative Weiss constant is suggestive of dominant antiferromagnetic exchange interactions in this region but the small value provides an element of uncertainty.

3.3. *Magnetic properties of RE_2CrSbO_7 (RE=Y, Tb, Dy, Er).*

To investigate the interactions between Cr^{3+} *B*-site ions without the presence of magnetic *A*-site cations, the compound Y_2CrSbO_7 was prepared and studied using SQUID magnetometry (Fig. 8). Y_2CrSbO_7 is reported in the literature to have ferromagnetic Cr–Cr interactions [10]. As for Ho_2CrSbO_7, inverse susceptibility plots revealed a transition at 143 K which was assigned to a very small $YCrO_3$ impurity [18,19]. The presence of a ferromagnetic

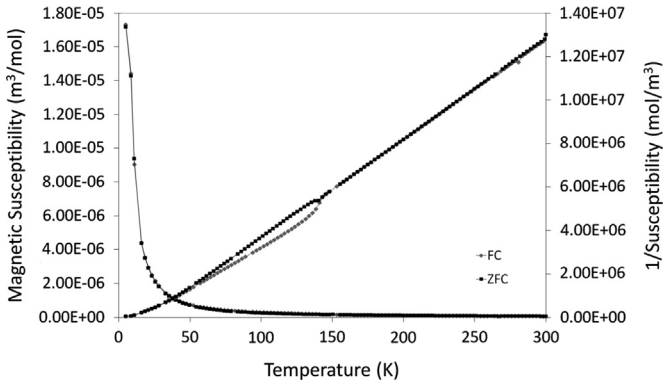

Fig. 8. Variation of magnetic susceptibility and inverse susceptibility with temperature for Y_2CrSbO_7 at an applied field of 500 Oe.

transition was not obvious from the susceptibility plot but hysteresis behaviour was observed at 5 K.

The presence of ferromagnetic Cr^{3+} ordering in Y_2CrSbO_7 at low temperatures indicates that the Cr^{3+} ion order is inherent in these systems and not due to the presence of magnetic lanthanide ions on the *A*-site. In fact, it is thought that the field provided by the ferromagnetic Cr^{3+} ions at low temperature is enough to lift the degeneracy of the *x*, *y* and *z* axes and induce ordering of the Ho^{3+} moments.

These results indicate that related materials containing *B*-site Cr^{3+} ions would show magnetic lanthanide ion ordering at low temperatures and the samples Tb_2CrSbO_7, Dy_2CrSbO_7 and Er_2CrSbO_7 were prepared.

The compound Dy_2CrSbO_7 has been reported to order magnetically below 16 K [10]. Transitions were seen in the susceptibility data for Dy_2CrSbO_7 at approximately 18 K and 150 K corresponding to ordering of the Dy^{3+} moments and $DyCrO_3$ impurity [19], respectively. Fitting the data to the Curie–Weiss law gave a total moment, $\mu_{total}=15.7\ \mu_B$ and a Weiss constant, $\theta=-6.0$ K. The moment is as expected for two Dy^{3+} ions ($\mu_{exp}=10.63\ \mu_B$) and one Cr^{3+} ion, and the Weiss constant is, again, indicative of antiferromagnetic behaviour. Hysteresis data collected at 5 K gave a saturated moment of 11.96 μ_B, showing that the Dy^{3+} moment is also reduced by the 111 anisotropy.

The high temperature transition attributed to *RE*CrO_3 impurity was also observed in the susceptibility data for Tb_2CrSbO_7 (at 161 K) and Er_2CrSbO_7 (at 139 K) [18,20].

4. Conclusions

The magnetic ordering in the pyrochlore Ho_2CrSbO_7 has been studied using neutron powder diffraction. Often magnetic ordering cannot occur in the frustrated magnetic sublattice of the pyrochlore structure but Ho_2CrSbO_7 forms an "ordered spin-ice structure" below 13 K where the Ho^{3+} moments are constrained along the ⟨111⟩ axes. Ferromagnetic ordering of the Cr^{3+} ions lifts the degeneracy of the *x*, *y* and *z* directions in the cubic structure and causes the ferromagnetic Ho^{3+} moment to align in one direction, unlike the spin-ice pyrochlores $Ho_2Ti_2O_7$ and $Dy_2Ti_2O_7$. The Cr^{3+} ions are therefore thought to be crucial for inducting magnetic Ho^{3+} ordering at low temperatures. At present, the precise nature of the Cr^{3+} interactions has not been established, and the effect the transition metal ion has on rare earth magnetic ordering provides interesting possibilities for further research.

Acknowledgments

We thank the EPSRC (EP/P504813/1) for financial support, Dr. Elizabeth Blackburn at the University of Birmingham, UK for her help with the analysis of SQUID magnetometry data and Vladimir Pomjakushin at the Paul Scherrer Institute (PSI) for his help with the collection of NPD data. The Bruker D8 diffractometer used in this research was obtained through Birmingham Science City: Creating and Characterising Next Generation Advanced Materials (West Midlands Centre for Advanced Materials Project 1), with support from Advantage West Midlands (AWM) and part funded by the European Regional Development Fund (ERDF).

References

[1] M.A. Subramanian, G. Aravamudan, G.V. Subba Rao, Prog. Solid State Chem. 15 (1983) 55–143.
[2] M.A. Subramanian, A.W. Sleight, in: K.A. Gschneidner Jr., L. Eyring (Eds.), Handbook on the Physics and Chemistry of Rare Earths, 16, Elsevier Science Publishers B.V, 1993, pp. 225–248.
[3] H. Sakai, K. Yoshimura, H. Ohno, H. Kato, S. Kambe, R.E. Walstedt, T.D. Matsuda, Y. Haga, Y. Ōnuki, J. Phys.: Condens. Matter 13 (2001) L785–L790.
[4] Z. Hiroi, J. Yamaura, S. Yonezawa, H. Harima, Physica C 460–462 (2007) 20–27.
[5] J.S. Gardner, M.J.P. Gingras, J.E. Greedan, Rev. Mod. Phys. 82 (2010) 53–107.
[6] S.T. Bramwell, M.J.P Gingras, Science 294 (2001) 1495–1501.
[7] M.J. Harris, S.T. Bramwell, D.F. McMorrow, T. Zeiske, K.W. Godfrey, Phys. Rev. Lett. 79 (1997) 2554–2557.
[8] L. Pauling, J. Am. Chem. Soc. 57 (1935) 2680–2684.
[9] C. Castelnovo, R. Moessner, S.L. Sondhi, Nature 451 (2008) 42–45.
[10] P.F. Bongers, E.R. Van Meurs, J. Appl. Phys. 38 (1967) 944–945.
[11] A.C. Larson, R.B.V. Dreele, General Structure Analysis System, , 1994 (Los Alamos National Laboratory Report LAUR 86-748).
[12] B.H. Toby, J. Appl. Crystallogr. 34 (2001) 210–213.
[13] Y. Su, J. Zhang, Z. Feng, Z. Li, Y. Shen, S. Cao, J. Rare Earths 29 (2011) 1060–1065.
[14] N. Taira, M. Wakeshima, Y. Hinatsu, A. Tobo, K. Ohoyama, J. Solid State Chem. 176 (2003) 165–169.
[15] I. Mirebeau, A. Apetrei, J. Rodríguez-Carvajal, P. Bonville, A. Forget, D. Colson, V. Glazkov, J.P. Sanchez, O. Isnard, E. Suard, Phys. Rev. Lett. 94 (2005) 246402/1–246402/4.
[16] K. Matsuhira, Y. Hinatsu, K. Tenya, T. Sakakibara, J. Phys.: Condens. Matter 12 (2000) L649–L656.
[17] C. Bansal, H. Kawanaka, H. Bando, Y. Nishihara, Physica B 329 (2003) 1034–1035.
[18] T. Morishita, K. Tsushima, Phys. Rev. B 24 (1981) 341–346.
[19] K. Tsushima, K. Aoyagi, S. Sugano, J. Appl. Phys. 41 (1970) 1238–1240.
[20] J.D. Gordon, R.M. Hornreich, S. Shtrikman, B.M. Wanklyn, Phys. Rev. B 13 (1976) 3012–3017.